INTERNATIONAL JOURNAL OF TECHNO-ENGINEERING
IJTE

ISSN: 2057-5688

Nuclear Reaction Experiments to Indirectly Examine Astrophysical Capture Reactions

N Kiranmai, Research Scholar, Department of Physics , J.S University, Shikohabad.

Dr.Vishnu Singh Rathore, Assistant Professor ,Supervisor, Department of Physics, J.S University, Shikohabad.

Abstract: Both nuclear physics and astrophysics are subfields of physics, but collectively they are referred to as "Nuclear Astrophysics." It does this by integrating star and other astrophysical system models with nuclear physics data such as the abundances of isotopes, their masses, how long their half-lives are, and the cross-sections of nuclear reactions. The study of the objects that can be seen in the universe is called astronomy. Validating and comprehending astronomical measurements, in addition to conducting research into the microscopic processes that take place within stars, are all tasks that need the use of nuclear astrophysics. Laboratory experiments are difficult, if not impossible, to do with the technology that is now available because the energy level at which the bulk of capture events occur in the stellar environment is so high. Using the indirect approach, many techniques have been developed for finding the cross-sections of this reaction and estimating the corresponding reaction rates. These techniques have also been developed. The purpose of this article is to get an indirect knowledge of astrophysical capture reactions via the investigation of a few experimental nuclear reaction methods. The purpose of the study is to make projections on astrophysical capture cross sections by using information obtained from nuclear reaction experiments.

Keywords-Nuclear, Physics, astronomy, Experiments.

1. INTRODUCTION

It is very necessary to have an understanding of the nuclear astrophysics-related neutron capture processes in order to appreciate the workings of metals that are denser than iron. become a reality. The component of the weak and accelerated s-process in massive stars known as the 68Zn(n,)69Zn capture reaction is the one that has the most influence on the overall quantity of 68Zn that is generated. The route for s-process nucleosynthesis, which is responsible for the generation of 68Zn, is harmed as a result of this reaction. However, this correlation between the amount of 68Zn and a specific reaction, 68Zn(n,)69Zn, was not established until quite recently [132]. According to Koloczek's most current compilation for the s-process nucleosynthesis [133], it was established that the abundance of 80Kr is very sensitive to the 68Zn(n,)69Zn capture reaction. This conclusion was reached based on the findings of a study. It was revealed

INTERNATIONAL JOURNAL OF TECHNO-ENGINEERING
IJTE
ISSN: 2057-5688

that this was the case.

The calculations of the statistical model (SM), which were used in the explanation of the neutron capture reaction, are utilized in order to arrive at an estimate of the frequency with which the astrophysical event takes place. For the purpose of calculating the reaction's cross-sectional area, the Hauser-Feshbach model is used. The model needs the nuclear level density (NLD) parameter, the ray strength function, and the optical model potentials (OMP) in order to determine the -ray transmission coefficients. As can be seen in Figure 1, the previous statistical model calculation of the 68Zn(n,)69Zn capture cross-section, which factored in a number of NLD prescriptions (including the Farmi Gas model, the Constant Temperature model, and the microscopic NLD of Goriely), resulted in an overestimation of the cross-section values of the available experimental data. This was due to the fact that the model took into account a number of NLD prescriptions. As a direct result of this too optimistic projection, we entertained the idea of removing the NLD of 69Zn from the experiment and instead using it as an input parameter in the SM calculation. This was done since the projection was excessively optimistic. Using this method, our goal was to limit the capabilities of the model to calculate the 68Zn(n,)69Zn capture cross-section.

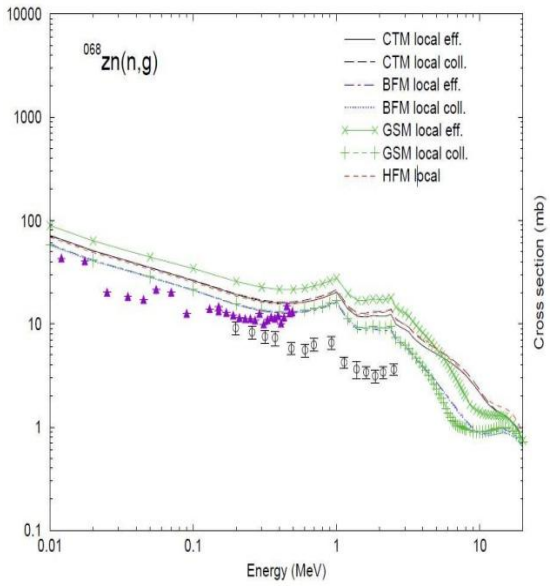

Figure 1:(Color online) The comparison of ^{68}Zn(n, γ)^{69}Zn capture data(triangular and circular points) with statistical model calculation considering different NLD prescription (Colorline).

2. Statistical Model Calculation For Fusion Evaporation Reaction

The basic premise of the statistical model is that a compound nucleus arises with an excitation energy high enough to allow for the excitation of numerous states by the interaction of projectile nucleons with target nucleons. This supposition is based on the fact that a compound nucleus forms with an excitation energy high enough to allow for the excitation of a compound nucleus. In addition, before the process of decay starts, all of the degrees of freedom, including mass, energy, and angular momentum, reach a state of equilibrium. The equilibrated compound nucleus decays without remembering how it was generated in the entrance channel, according to Bohr's theory, with the exception of preserved variables such as excitation energy, angular momentum,

INTERNATIONAL JOURNAL OF TECHNO-ENGINEERING
IJTE
ISSN: 2057-5688

parity, and isospin. This is the case even when other variables are maintained.Evaporation of particles (n, p, and) and emission of particles are the two fundamental processes that lead to the decay of compound nuclei.

CASCADE:statisticalmodelcalculationcode

The statistical model code known as CASCADE may be used to make a prediction about the decay of a complex nucleus that has been subjected to a nuclear reaction. It wasn't until 1977 that Puhlhofer came up with the concept, but since then, a great deal of work has been done by other scientific groups to modernize, adapt, or otherwise enhance the code so that it better serves their needs. A significant component that goes into the construction of the code is the Hauser-Feshback formalism of compound nucleus statistical decay. Together, the beginning excitation energy (E*) and the distribution of angular momenta (J) in the form of a matrix called (E*, J) serve as a description of the outgoing CN and are used to determine the CN decay probabilities. After Following the completion of the calculations necessary to determine the neutron probability, proton probability, and fission probability for each matrix element, the relevant populations are relocated to new matrices denoted by the symbols (E*, J). These brand new matrices include data that was not accessible in the past. This process is repeated a number of times until the energy of the ejected nucleus has been decreased to a level that is lower than the particle threshold. The compound nucleus finishes the process by first emitting a statistical ray with energy lower than the particle threshold, then switching to a new (E*, J) matrix and emitting a low energy discrete yrast ray. Finally, the particle threshold is crossed, and the process is considered successful. Before the compound nucleus releases a low energy discrete yrast -ray, all of these stages take place one after the other. The initial population is used as the basis for the calculation of the program that determines the energies of evaporating neutrons, protons, and rays. The nuclear level density, also known as NLD, and the risk of decapping are the two primary components that went into the creation of the statistical modely.

Decay probabilities

Compound nuclei that have a high excitation energy and lose their angular momentum by the emission of particles (often either n, p, or rays).The reciprocity theorem is used in the process of computing the statistical significance of the beginning and final states, in addition to transmission coefficients (barrier penetrability), which play a role in determining the probability of particle emission. The equation that describes the decay rate Rp of a particle that was expelled from a nucleus that had been extinguished (atexcitationenergyEi,spinJi,parityEi) in order to form a nucleus that was decaying (atEf,Jf,f) may be written as follows:

$$R_p d\epsilon = \frac{\rho_f(E_f, J_f, \pi_f)}{2\pi\hbar\rho_i(E_i, J_f, \pi_i)} \sum_{S=J_f-s_p}^{S=J_f+s_p} \sum_{L=J_i-S}^{L=J_i+S} T_L^p(\epsilon_p) d\epsilon_p$$

p represents the amount of kinetic energy possessed by the particle. The emitting particle's binding energy, spin, and orbital angular momentum, sometimes referred to as Bp, are represented by the symbols sp and L, respectively. The symbol for the nuclei's initial level densities is an i, whereas the letter f stands for the final level densities of the nuclei. The coefficient of transmission of an energy particle is denoted by the letter Tp. Before

INTERNATIONAL JOURNAL OF TECHNO-ENGINEERING
IJTE
ISSN: 2057-5688

attempting to calculate the particle transmission coefficients, it is necessary to first solve the optical model equations that describe the nuclear system. During this experiment, we will be searching for alpha particles that are in the process of dissipating.

Nuclear level density

Thebasicnuclearleveldensityformula,which iswidelyusedinstatisticalmodelcalcu-lation,derivedfromtheFermigasmodel,base donthepioneeringworkofBetheisgivenby prescription of level density parameter *a*, which takes into account theshelleffectsasafunctionofexcitationener gy,isadoptedanditisexpressedas

$$\rho(E^*, J) = \frac{2J+1}{12\theta^{3/2}}\sqrt{a}\frac{exp(2\sqrt{aU})}{U^2}$$

$$a = \tilde{a}[1 + \frac{\delta S}{U}[1 - \exp(-\gamma U)]]$$

where,$\tilde{a}$=A/*k*and*k*isinverseleveldensitypara meter.δSisground-stateshellcorrection definedasthedifferenceoftheexperimentalan dtheoretical(liquiddrop)masses.γ^{-1}=$0.4A^{4/3}$ istherateatwhichtheshelleffectisdampedwitht heincreaseinexcitationenergy.Themomentofi nertiaoftheCNistakenasI_{eff}=$I_0(1+\delta_1 J^2+\delta_2 J^4)$, where$I_0$(=$^2MA^{5/3}r^2$)isthemomentofinertiaofas phericalnucleus.$\delta_1$and$\delta_2$arethedeformability50parameters,$r_0$istheradiusparameterand*J*isthet otalspinofthenucleus.

Hausher-Feshback modeling of (n, γ) capture reaction

When attempting to define neutron capture processes, one method used to arrive at an approximation of the astrophysical reaction rate is to do calculations based on statistical models. When calculating the reaction cross-section, the Hauser-Feshbach model is what's often utilized. Optical model potentials, often known as OMP, are a must if one wants their model to appropriately depict particle transmission.

subsequent neutron capture, nuclear level density (NLD), gamma-ray strength function, and coefficients for estimating the -ray transmission coefficients of the composite nucleus are all included in this calculation.

Optical model potential

According to the optical model, it is possible to use a sophisticated mean-field potential to mimic the precise interaction that takes place between an input particle and a nucleus. This interaction takes place when an input particle collides with a nucleus. This assertion is confirmed by the optical model's correctness, which has been tested. The response flux is split into two parts by this intricate mean-field potential: one part accounts for all of the competing non-elastic channels, while the other part accounts for shape elastic scattering. The topic of shape dispersion is covered in both of these sections. The Schrodinger equation may be quantitatively solved in light of these complex possibilities, which will provide a wealth of knowledge that is helpful in many different contexts. The first thing that it does is the basic observable, which includes the elastic angular distribution and polarization, the reaction and total cross-section, and, at low energies, the s-wave and p-wave strength functions, as well as the potential scattering radius R'. This is the first thing that it accomplishes. It makes projections based on this observable. Additionally, it forecasts the response in addition to the overall cross-sectional area. The formation cross-section of the composite nucleus is computed with the help of the s-wave strength function and the p-wave strength

ISSN: 2057-5688

function.

The power of the ray function

The gamma emission channel of the nuclear process may be defined with the help of gamma-ray transmission coefficients. Because gamma rays often duplicate the route taken by the emission of any other form of particle, this path is fairly common. In the same manner that the particle transmission coefficients supplied by the optical model are utilized to compute the competition between photons and other particles, the Hauser-Feshbach model also incorporates gamma-ray transmission coefficients. In the event where X equals M or E, the following formula may be used to determine the multipolarity l of the gamma-ray transmission coefficient for type X.

Gamma energy is denoted by the letter E, and the energy-dependent gamma-ray strength function is denoted by the symbol fXl(E). When calculating the gamma-ray intensity function, many different models were used. For the sake of this computation, we make use of the Brink-Axel option for any transition type that isn't E1 and any transition type that happens after E1.

3. EXPERIMENTAL DETAILS

In June of 2018, a research was conducted at the BARC-TIFR PelletronLinac Facility in Mumbai, India. The objective of the research was to produce a metallic 64Ni that could maintain its own existence and was enriched to 99%. Oak Ridge National Laboratory in the United States supplied the target, which has a thickness of about 507 10 g/cm2 and was used in the experiment. A method referred to as charge particle energy loss has been used up to this point in order to determine the thickness of the target. The target 64Ni was struck by a stream of 9Be particles traveling at 30 MeV, which resulted in an increase in the excitation energy of the compound nucleus 73Ge to 41.8 MeV.

Detector setup and data acquisition

Thedetectorsetupconsistsoftwomajordetector systemswhicharegivenbelow:

The CsI(Tl) detector forde tecting evaporated light charged particle (α,proton) from the compound nucleus(CN).

Table1:OrientationofthedetectorsinING Aarray

Pocket No.	Distance from target (in cm)	Polar angle (θ) (in deg.)	Azimuthal angle (φ) (in deg.)
1	25	157	0
2	25	157	120
3	25	157	240
4	25	140	60
5	25	140	180
6	25	140	300
7	25	115	150
8	25	115	270
9	25	90	120
10	25	90	180
11	25	90	240
12	25	90	300
13	25	40	60
14	25	40	300

The INGA set up for detecting de-exciting discrete γ-rays from the residual nu-cleus. Because of its spherical shape, the INGA array has the potential to accommodate the installation of as many as twenty-four clover detectors. The clover detector crystal is situated at a distance of 25 centimeters from the center of the target. The goals of the investigation are laid forth in Table 1, which details where the clover

INTERNATIONAL JOURNAL OF TECHNO-ENGINEERING
IJTE
ISSN: 2057-5688

detectors should be placed. A tiny spherical chamber with a diameter of 20 centimeters was needed in order to accommodate the CsI(Tl) detectors and target frames that are shown in the right panels of Fig. 4.2. In order to identify the emitted charged particles, CsI(Tl) detectors were used. These detectors had dimensions of 15 millimeters by 15 millimeters and a thickness of 3 millimeters. Two different sets of detector combinations were put in positions that were symmetrical with respect to the beam axis and were five centimeters apart from the precise center of the target. The detectors were arranged such that one would be on each side of the beamline in order to cover an annular area on the reaction plane that varied in size from 22 to 67. Prior to the development of CsI(Tl) detectors, the blocking of the entry of elastically dispersed particles was accomplished by using tantalum absorbers with a thickness of 30 mg/cm2. 14 artists influenced by Compton Clover detectors are dispersed around the whole of the INGA detecting system in a circular pattern at a variety of different angles to the beam stream. Two of these angles have a measurement of 40 degrees, four of them have a measurement of 90 degrees, two of them have a measurement of 140 degrees, two of them have a measurement of 115 degrees, and four of them have a measurement of 157 degrees. Figure 2 provides a more in-depth look at the detector's physical configuration.

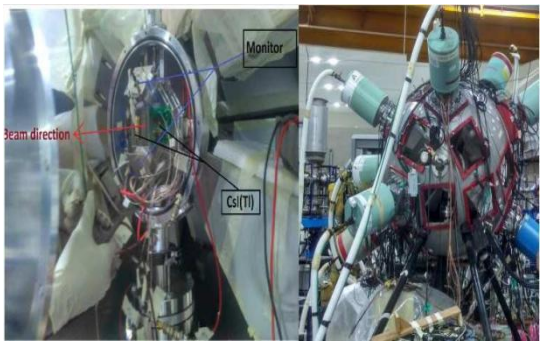

Figure2:PictureofdetectorsetupatTIFR-BARCPelletronLinacFacility.

It was decided to use a digital data acquisition system (DDAQ) that was based on XIA-LLC Pixie-16 modules in order to capture data using the list mode. These modules were accountable for giving both time and energy information to the system. At a sampling rate of 100 MHz, this apparatus is able to digitize 96 channels that are made up of 24 Clover detectors, as well as 16 channels that are made up of 16 CsI(Tl) detectors. It is able to function in a mode that is dependent on triggers as well as a mode that involves multiple coincidences. The BGO signals emitted by the anti-Compton shields of the different clovers were able to suppress the channels that were being investigation. Singles mode was used to capture the data, and a time stamp was obtained for each distinct occurrence. For the purpose of particle identification, both the short gate integrated charge and the long gate integrated charge pulse shape characteristics of CsI(Tl) detectors were successfully realized.

Data analysis

Using the multiparameter time-stamped based coincidence search engine (MARCOS), [145] the raw data was arranged and sent in a manner that was compatible with Radware and root. Independent calibrations of the CsI(Tl)

ISSN: 2057-5688

detector and the clover detector were carried out with the use of the sorted data.

CloverDetectorCalibration

In every HPGe crystal that makes up a clover detector, there is an Analog to Digital Converter (ADC) that is responsible for digitizing the incident ray energy. If there is no offset, the ratio of the energy of the beam that has just made contact with it to the total number of channels in the ADC will be proportionate. Crystals in the clover detector have a very variable effect on the gain obtained by the detector. As a result of this, it is very important to connect the channel to the energy by using radioactive sources that have been granted permission to serve as the connecting medium. We used 152 Eu and 133 Ba as reference sources so that we could calibrate the energy. A quadratic equation was used to describe the data after it was established that there was a connection between the amount of x-ray energy and the channel numbers for both the 152Eu and 133Ba sources.
The expression for E(keV) is a0 plus a1 x plus a2 x 2, where x represents the number of channels and ai-s refers to the calibration constants. Figure 3 shows the raw spectra of the four clover crystals as well as the spectra of the crystals after their gains have been matched. These spectra are shown side-by-side for comparison. After gain matching, the energy peaks of four different crystals coincide, demonstrating that the calibration was successful. This is seen in Figure 3.

Only the counts of light peaks that were created by photoelectric absorption may be added together when using the add-back mode of a clover detector. The energy spectrum of each crystal is combined as a result. As can be observed by combining the correlated events in the two surrounding crystals, the events that are Compton diffused from one crystal and absorbed in the next crystal also contribute to the overall peak energy value. This can be seen by putting the two crystals together. As a direct result of this, the peak energy number now takes into account the photoelectric events produced by all four crystals in addition to a portion of the Compton events. An add-back mode is the name given to this specific sort of mode. A comparison of the add spectrum and the add-back spectrum for a single clover is shown in Figure 4. Comparison is made between the Eu and Ba decay lines. In addition to this, the add-back factor for the area extending from E 82 to 1408 keV is calculated. The ratio of the total add-back counts to the total photopeak counts is what the add-back factor measures. Figure 5 makes it very evident that, as was to be anticipated, the low energy factor is rather near to one. The factor rises with increasing -ray energy until it reaches these intermediate energies, which occurs when the probability of Compton scattering is equal to that of the photoelectric effect and the add-back mode starts to participate.

INTERNATIONAL JOURNAL OF TECHNO-ENGINEERING
IJTE
ISSN: 2057-5688

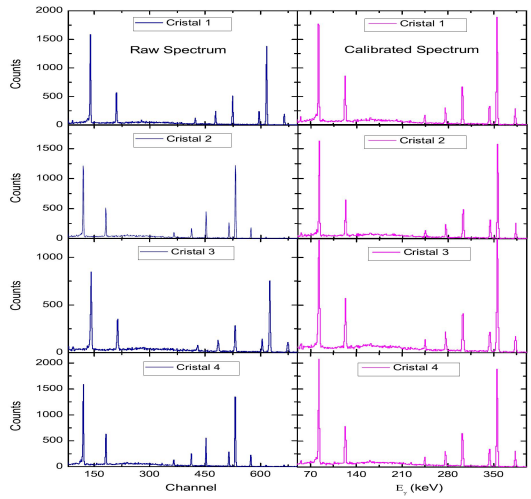

Figure3:Acomparison of the calibrated spectrum with their respective raw spectrum of the four crystals of acloverfor^{152}Euand^{133}Basources.

Particle identification nusing CsI (Tl) Detector

During the course of the live experiment, we were able to record two and a half shape parameters of CsI(Tl) signals. This was previously mentioned.

An integrated charge may call a short gate at any point in time between t=0 and tmax, with the moment when the signal height is at its highest being denoted by the variable tmax.

There is no net accumulation of charge between the long gate and time t; this is represented by the value zero.
The comparison of the Qlong and Qshort components of the 2D spectrum is displayed presently. Because it is a two-dimensional spectrum, we were able to identify all of the different proton bands, as seen in Figure 8. In addition, we make use of data obtained from a 229Th source; as a consequence of this, the QDC spectrum shown in Figure 6 is comparable. Following the procedure of plotting the channel numbers of Qlong against the locations of the energy peak for 229Th sources, the quadratic equation shown in Figure 7 was applied to the data in order to get a satisfactory match. Adjust the QDC channels so that they have the same amount of energy as the live data.

using quadratic equations for particles right now.

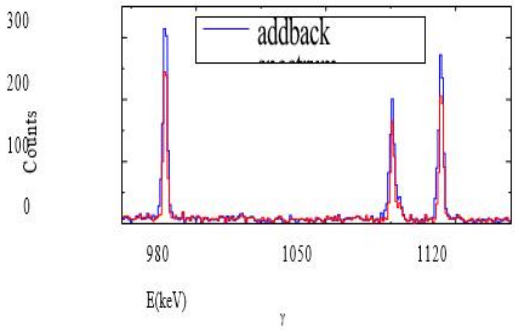

Figure4:A comparison of add and add-back spectrum of one clover.

ThecoincidencematrixbetweenCSI(Tl)andc loverdetectorevent. Save this coin in a format that a root file can understand after you're finished. Within the context of the root program, a more in-depth data analysis has been carried out. In order to determine the -events that were generated by the CsI(Tl) detectors, a method known as plus shape discrimination was used. The matrix of events related with coincidental occurrences is shown in Figure 9, where the -energy E is set up against the energy E. In Figure 9, you'll see not only the projected spectra of the E vs. E matrix, but also a number of other channel transitions that have been observed. In the course of the investigation, these lines were used in order to acquire gated spectra for a particular residue that was related to the decay channel.

Extraction of evaporated α-spectra from

INTERNATIONAL JOURNAL OF TECHNO-ENGINEERING
IJTE
ISSN: 2057-5688

CN decay

Themainaimofthispresentworkistoextractth eNLDof^{69}Znanduseittocalculatethe^{68}Zn(n, γ)^{69}Zn capture cross-sections. In this section, we discuss the extraction processofNLDfromγ-gatedα-spectra.WhileextractingtheNLDsfromthepa rticleevaporationspectrum, it is to be ensured that the contributions from non-compound processes are neg-ligiblysmall.Thisisthepre-requisitefortheextractionoftheNLDparamet erbyparticleevaporation technique. To select out the purely compound events, the γ-decay (E_γ= 332and 152keVof^{68}Zn) oflowest-lyingnegativeparity states6$^-$and 8$^-$havebeen chosen

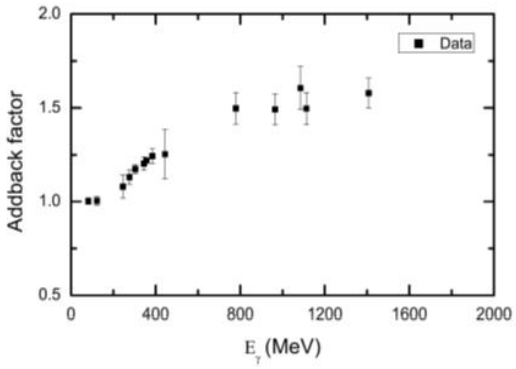

Figure5:The variation of add-back factor with energy of γ-rays.

the spectrum leading up to the gate. It is It is important to point out that the level scheme for 68Zn that was achieved via the use of the coincidence matrix in this experiment is consistent with the level scheme that was published in reference. Direct production of the nucleus 68Zn is possible by nuclear disintegration of the composite nucleus 73Ge, whereas indirect production may occur through partial fusion of 9Be with 64Ni and the transfer of the 5He fragment from 9Be to 64Ni. The synthesis of 68Zn becomes more likely once a piece of 9Be is directly transferred to the bound excited states of 68Zn. It's possible that the CN decay will take place in the states with even spin and odd parity 6 and 8 that are present in the 68Zn residue. Due to the fact that the parity is odd, these even spin, odd parity states cannot be filled by performing a simple transfer from 0+ to 64Ni(0+). If a heavier 5He fragment with a Q-value of +10.24 MeV is transferred from 9Be, then the ejected kinetic energy will be in the range of 36.0 to 39.5 MeV, covering the measured angular region of 22 to 67. This is because the Q-value of the heavier 5He fragment is greater than the Q-value of 9Be. This is the case regardless of the perspective that is being taken into account. The energy of the breakdown, which represents the partial fusing of the 5He target and the 64Ni source, will still fluctuate between 8 and 12 MeV. This is because the energy reflects the partial fusion of the target and the source. Because of this, other reaction pathways than the CN process that have kinetic energies higher than 12 MeV will not have any impact on the reported gated-particle energy spectrum. The gated energy spectra are shown in Fig. 12's upper and lower panels, respectively. The spectra are converted into the CM frame so that a comparison may be made between the observed findings and the predictions made by the statistical model, and so that the behavior of NLDs can be investigated in relation to the amount of energy used to excite them.

INTERNATIONAL JOURNAL OF TECHNO-ENGINEERING
IJTE
ISSN: 2057-5688

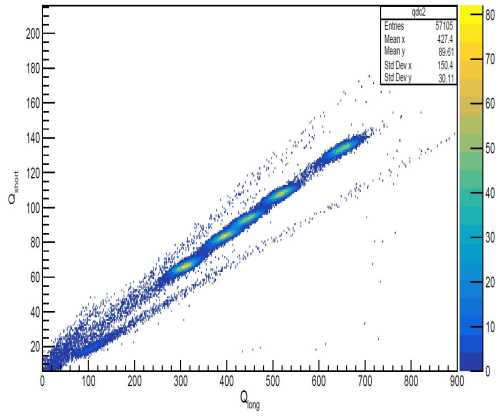

Figure6:(Coloronline)QDCspectrumof CsI(Tl)for^{229}Thsource.

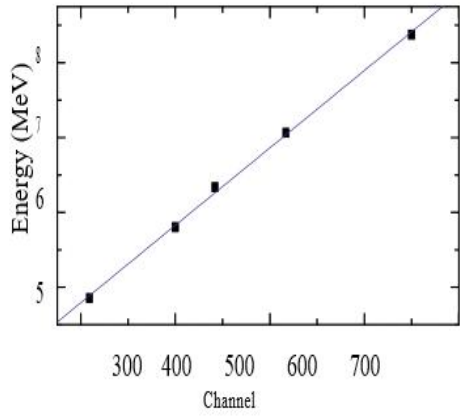

Figure7:(Coloronline)Calibrationcurvef oraCsI(Tl)detector.

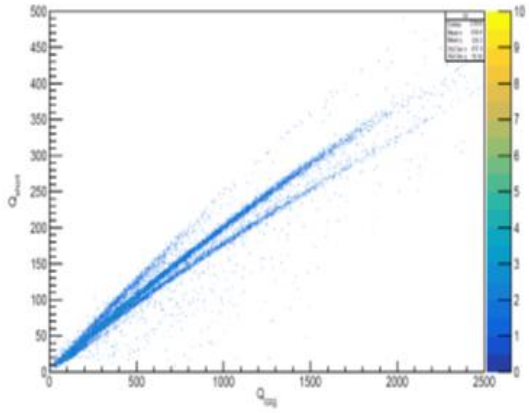

Figure8:(Coloronline)QDCspectrumof CsI(Tl)for^{9}Be+^{64}Nireactionat30MeV.

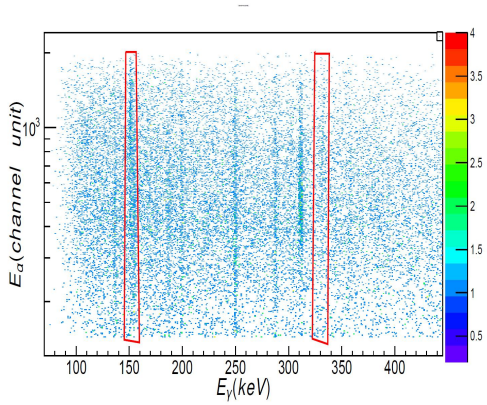

Figure9:(Coloronline)α-γcoincidencematrixextractedfromrawpa rticle-γmatrix.Theevents ofinterestarebounded by solid redboxes.

Extraction of level density parameter a(S n) and calculation of 68Zn(n, γ)69Zn capture cross-section

In addition, the nucleus level density parameter a for 69Zn is figured out by using Eq. 4.3's recovered inverse level density parameter k as a guide. For the purpose of this computation, the neutron separation energy S n was used. Using the equation U(Sn) = S n = 5.114 MeV computed from S n = 6.48 MeV, S = 1.368 MeV, and S = 3.37 MeV from Reference [156], we were able to determine that a(S n) = 8.625 0.225, which is in agreement with the findings that Dilg et al. got for this nucleus. Dilg et al. came at this conclusion, and it fits very well with what they discovered about this nucleus. After doing more research, scientists decided to employ the value provided by the TALYS1.9 nuclear reaction algorithm in order to develop the 68Zn(n,)69Zn capture cross-section.The TALYS computer software uses the NLD Fermi gas model as its primary data source. Only the E1 strength function, which has a generalized Lorentzian shape, has been investigated in

INTERNATIONAL JOURNAL OF TECHNO-ENGINEERING
IJTE
ISSN: 2057-5688

the neutron capture process that is largely of the E1 kind. The global neutron optical model potential was used during the construction of the statistical model. For the mass range of 24 A 209 and the energy range of 0.001 MeV to 200 MeV, this model potential is valid [159]. every additional variableThe code stays the same throughout, with the exception of a parameter that controls the nuclear level density. This figure was determined by using the findings of the most recent measurement that was performed. It is essential to keep in mind that, as shown in Figure 14, the reaction cross-sections produced from TALYS calculations using the observed NLD value explain the supplied data in a reasonable and effective manner, eliminating the need for any further normalization. This fact is illustrated. It is essential that you keep this in mind. The calculation that employed the systematic value of the NLD parameter a(S n)=9.614 [136] made a prediction that the results in the energy measurement area would be substantially higher than what was found. However, the findings are significantly lower than what was expected. It has been determined that the Maxwell-Avarage cross-section (MACS) and the 68Zn(n,)69Zn reaction rate are both functions of the temperature of the star. We are now at the very end of our journey.

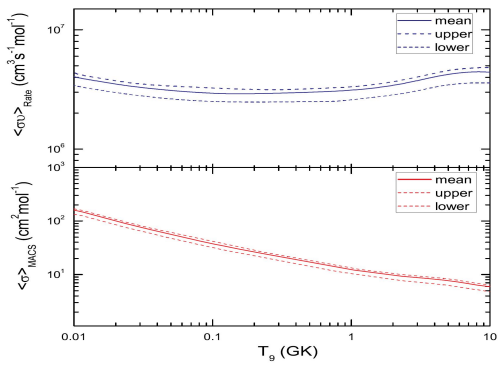

Figure15:TheracationrateandMACScross-sectionvariationwiththestellertemperatureof^{68}Zn(n,γ)^{69}Zncapturereaction.

CONCLUSION

At low energies (E = 152 and 332 keV), the -gated alpha emission spectra of the reaction 9Be + 64Ni were seen. Because of the even spin, odd parity (6 or 8), and decaying states in 68Zn, which is the surviving nucleus from the decay of the compound nucleus 73Ge, the majority of the -gated alpha energy spectra come from compound nuclear events. This is due to the fact that 68Zn is the nucleus that was left over after the decay of 73Ge. The production of 68Zn results from the dissolution of the composite nucleus 73Ge. The level density of the 69Zn nucleus as a function of excitation energy has been measured by comparing the observed alpha energy spectra with the expected values derived from the statistical model. This comparison was carried out in order to arrive at the results. The density of the level was established by this comparison. In order to calculate the 68Zn(n,)69Zn capture cross-sections, the TALYS method was used, and the NLD parameter that was produced as a consequence was assessed while the neutrons were kept apart. The aim of empirically restricting the parameters of the statistical model in order to provide a more accurate representation of the astrophysical events has been achieved as a result of the good agreement with the observed (n,) cross-section. This was accomplished as a result of the great agreement.

REFERENCES

[1] Banu,L.Trache,F.Carstoiu,N.L.Achouri,*etal.*,Phys.Rev.C2010,84,015803(1-7).
[2] F.M.Nunes,G.Potel,T.Poxon,andJ.

ISSN: 2057-5688

A.Cizewski,Ann.Rev.Nucl.Sci.20 20,70.,147-172.
[3] Spitaleri, M. Aliotta, S. Cherubini, M. Lattuada, *et al.*, Phys. Rev. C 1999, 60.,055802(1-7).
[4] Tumino,C.Spitaleri,MLaCognata, SCherubini,*etal.*,Nature2018,557., 687-690.
[5] M.LaCognata,C.Spitaleri,A.Mukha medzhanov,A.Banu,*etal.*,Astrophys. J.2010,708.,796-811.
[6] S.Cherubini,M.Gulino,C.Spitaleri, G.G.Rapisarda,*etal.*,Phys.Rev.C2 015,92.,015805 (1-7).
[7] R.G.Pizzone,M.LaCognata,L.L*et al.*,Eur.Phys.J.A2016,52.,77(1-9).
[8] A.M.Mukhamedzhanov,Phys.Rev. C2011,84.,044614.
[9] C.A.Bertulani,M.S.HusseinandS.T ypel,Phys.Lett.B2018,776.,217-221.[63]G.Baur,Phys.Lett.B1986,1 78.,135-138.
[10] G.Baur,C.BertulaniandH.Rebel, Nucl.Phys.A1986,458.,188-204.
[11] http://fpsalmon.usc.es/genp/doc/n uclear/experiments/s223/coulomb.s html.
[12] A.V.Voinov,S.M.Grimes,A.C.Lar sen,C.R.Brune,Phys.Rev.C2008,77. ,034613(1-6).
[13] J.Escher,LAhle,LBernstein,JBur ke,*etal.*,J.Phys.G2005,31.,S1687-S1690.
[14] J.E.EscherandF.S.Dietrich,Phys. Rev.C2006,74.,054601(1-16).
[15] ThomasRauscher.PhysicalReview C2010,81.,045807(1-8).
[16] J.Jose and M.Hernanz, Astro-phys.J.1998,494.,680-690.